

A Novel Maximum Distance Separable Coded OFDM-RIS for 6G Wireless Communications

Yiqian Huang, Ping Yang, *Senior Member, IEEE*, Bo Zhang, *Member, IEEE*, Zilong Liu, *Senior Member, IEEE*, Ming Xiao, *Senior Member, IEEE*.

Abstract—The vision of the sixth generation mobile communication (6G) calls for extremely reliable data transmission over complex and diverse wireless channels. By combining the maximum distance separable (MDS) codes with the classic orthogonal frequency division multiplexing (OFDM), we present a new paradigm with the assistance of the reconfigurable intelligent surfaces (RIS). In our design, the RIS with limited phase shifts are adopted and the pairwise error probability (PEP) of the proposed system is first derived. Then, in order to further minimize the bit error rate (BER), we provide a novel method based on phase alignment to obtain the optimal solution for the discrete phase shifts. Our simulation results show that the proposed scheme provides considerable BER performance improvements compared to conventional OFDM systems. Moreover, the proposed discrete phase optimization algorithm is capable of achieving performance similar to that of the system with continuous phase shifts.

Index Terms—Discrete phase shifts, MDS code, OFDM, RIS.

I. INTRODUCTION

THE ever growing use cases and data services in the sixth generation (6G) mobile networks have posed a number of challenges to traditional waveforms, which is one of the core components of the physical layer (PHY) design [1]. Aiming for ultra-reliable, spectrum- and energy- efficient wireless communications, extensive investigations have been carried out to design new waveforms for 6G [2][3].

Orthogonal frequency division multiplexing (OFDM) is the dominant waveform in current wireless communication systems (e.g., LTE, 5G New Radio, and Wifi) and is still recognized as a competitive waveform of 6G due to its efficient hardware implementation, robustness to multipath fading as well as single-tap equalization [4][5]. However, it is sensitive to frequency dispersion and hence OFDM alone may not be able to meet the stringent reliability requirements for future radio systems. This stimulates numerous efforts for improving the error rate performance of OFDM [6]-[8], including the combination with some coding and modulation techniques. For example, [9] combined index modulation (IM) with OFDM for exploiting the multi-domain benefits, while [10] integrated the

polar code with OFDM for their joint gains. Very recently, two maximum distance separable (MDS) code based modulation schemes were developed and combined with OFDM in [11]. The bit error rate (BER) performance of MDS based modulation schemes were proved to be attractive, since the MDS code integration helps increase the minimum Hamming distance between modulation symbols [12].

In view of the complicated channel conditions in future communication systems, reconfigurable intelligent surface (RIS) is widely regarded as a powerful technique for post-Shannon communication performances [13]. By integrating RIS with traditional OFDM systems, such as two-way OFDM and multi-antenna OFDM, researchers demonstrated that RIS is effective for improving system error performance [14]-[16]. Since OFDM can address multipath fading, MDS code can deal with burst errors, while RIS is able to improve the propagation environments, the combination and joint optimization of these three are worthy a close investigation. Moreover, the existing studies generally assume that the RIS phase shifts are continuous. It was pointed out in [17] and [18] that it is desirable for RIS phase shifts to be discrete for efficient practical hardware implementation. While this brings new design challenges, it is interesting to analyze the impact of discrete phase shifts and optimize the system with discrete phase shifts. Furthermore, more comprehensive and complicated RIS-phase shift models were proposed in [19] and [20], which were useful for hardware implementation of RIS.

In this letter, we propose a practical design paradigm for MDS coded OFDM-RIS systems. More specifically, we first design an MDS code based amplitude and phase modulation (MDS-APM) scheme, which combines MDS coding into signal modulation. Then, the proposed MDS-APM scheme is integrated into an OFDM system for a communication channel assisted with a practical RIS. Aiming for minimizing the BER, we deduce the pairwise error probability (PEP) of the proposed MDS-coded OFDM-RIS system. Then the expression of the optimal discrete RIS phase shifts is derived and a simple searching algorithm is developed. Numerical results indicate the effectiveness of the proposed framework in terms of significantly improved BER performance.

II. SYSTEM MODEL

This section describes the proposed system model as shown in Fig. 1. At the transmitter, MDS-APM is first conducted for the input bits. Subsequently, we perform OFDM modulation, which includes the inverse fast Fourier transform (IFFT) and cyclic prefix (CP) insertion. The OFDM signals are then transmitted over the RIS channel. After that, the scattered signals pass through independent and identically distributed wireless channels before they reach the receive antenna.

Y. Huang and P. Yang are with the National Key Laboratory of Science and Technology on Communications, University of Electronic Science and Technology of China 611731, Sichuan, China (e-mail: 202121220226@std.uestc.edu.cn, yang.ping@uestc.edu.cn).

M. Xiao is with the Department of Information, Science and Engineering (ISE), School of Electrical Engineering, KTH, Sweden (e-mail: mingx@kth.se).

B. Zhang is with Artificial Intelligence Research Center, National Innovation Institute of Defense Technology, Beijing, P. R. China (zhangbo10@nudt.edu.cn).

Zilong Liu is with the School of Computer Science and Electronics Engineering, University of Essex, Colchester, Surrey CO4 3SQ, U.K. (e-mail: zilong.liu@essex.ac.uk).

This work is supported by the National Key R&D Program of China under Grant 2020YFB1807203 and the National Science Foundation of China under Grant 61876033.

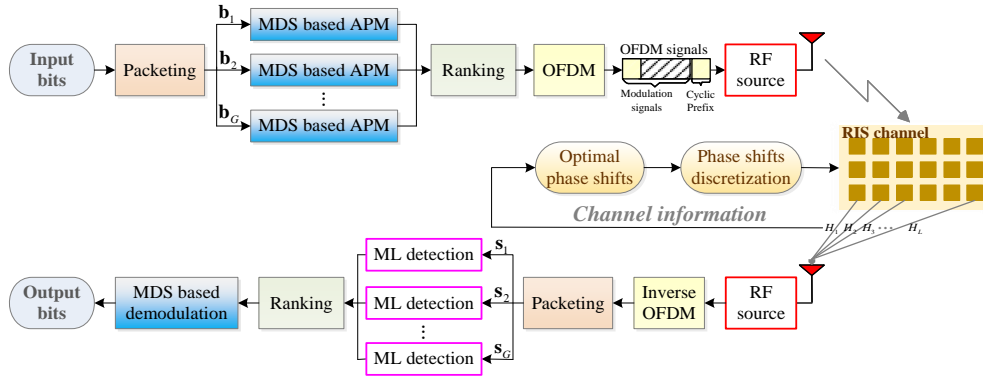


Fig. 1. System model of the proposed MDS-OFDM architecture with discrete RIS phase shifts.

The receiver conducts the inverse OFDM operations first. For an N -dimensional transmit signal $\mathbf{x} = [x_1, x_2, \dots, x_N]^T$, the receive signal at time slot $t, t \in \{1, 2, \dots, N\}$ is

$$y_t = \sum_{i=1}^F h_{it} r_{it} x_t + n_t, \quad (1)$$

where F denotes the number of the programmable reflectors in RIS. $x_t \in \mathbf{x}$ is the transmit signal at time slot t , h_{it} and r_{it} denote the i -th channel and i -th phase shift, respectively. n_t denotes the additive white Gaussian noise (AWGN). The distribution of n_t is $\mathcal{CN}(0, N_0)$, where N_0 is the noise variance. From (1), we can obtain the following expression for N -dimensional receive signals $\mathbf{y} = [y_1, y_2, \dots, y_N]^T$ as follows.

$$\mathbf{y} = \sum_{i=1}^F \mathbf{H}_i \mathbf{R}_i \mathbf{x} + \mathbf{n}, \quad (2)$$

where $\mathbf{H}_i = \text{diag}[h_{i1}, h_{i2}, \dots, h_{iN}] \in \mathbb{C}^{N \times N}$ is the i -th channel matrix and $\mathbf{R}_i = \text{diag}[r_{i1}, r_{i2}, \dots, r_{iN}] \in \mathbb{C}^{N \times N}$ is the i -th phase shift matrix. $\text{diag}[\cdot]$ denotes the diagonal matrix operator. $\mathbf{n} = [n_1, n_2, \dots, n_N]^T \in \mathbb{C}^{N \times 1}$ is the N -dimensional noises. For \mathbf{y} , the maximum likelihood (ML) detection is formulated as

$$\hat{\mathbf{x}} = \underset{\{\mathbf{V} \in \mathbb{V}\}}{\text{argmin}} \left\| \mathbf{y} - \sum_{i=1}^F \mathbf{H}_i \mathbf{R}_i \mathbf{V} \right\|^2, \quad (3)$$

where \mathbb{V} denotes the set of all possible combinations of modulation signals. Afterwards, the detected signal $\hat{\mathbf{x}}$ is demodulated and decoded based on the MDS concept successively, in order to obtain the estimated values of the input bits.

A. MDS based APM Scheme

1) *MDS Coding Scheme*: In MDS encoding scheme, each element can be between 1 and any positive integer Z . And the MDS coding mechanism follows the idea of check code in order to maximize the minimum Hamming distance between different symbols. Specifically, the MDS codes exploit the last codeword as the check code. For M -dimensional MDS codes $\{I_1, I_2, \dots, I_M\}$, the check code I_M is calculated by

$$I_M = Z - (I_1 + I_2 + \dots + I_{M-1}) \bmod Z, \quad (4)$$

where $\bmod Z$ represents module Z operation.

2) *Proposed MDS-APM scheme*: In the proposed framework, we develop the following simple principle to map the input bits into their corresponding MDS codes. For a binary sequence, we start with converting every $\log_2 Z$ bits into a decimal number between 0 and $Z - 1$. As the MDS encoding mechanism requires elements to be between 1 and Z , we further add 1 to each codeword. At last, the check code is calculated by (4). In general, for M -dimensional MDS codes, the first $M - 1$ codewords are determined by the binary sequence and the last codeword is determined by (4). Therefore, the length of the binary sequence that determines M -dimensional MDS codes is $(M - 1) \log_2 Z$.

After MDS coding, APM is applied to the subcarriers according to the corresponding MDS codes. In the proposed APM scheme, N subcarriers are first divided into G groups, and each group has $n = N/G$ subcarriers. For each group, the amplitudes and phases of the first $n - 1$ subcarriers are determined by the information bits, and the last subcarrier carries the check information. Assuming the orders of amplitude modulation (AM) and phase modulation (PM) are A and P , respectively, and the length of information bits that can be carried by N subcarriers (denote by L) is

$$L = G(n - 1)(\log_2 A + \log_2 P) = G(n - 1) \log_2 AP. \quad (5)$$

As can be seen from (5), the MDS-APM scheme requires the number of bits to be the power of 2.

For the g -th group, $g \in \{1, 2, \dots, G\}$, the amplitudes $[A_1^g, A_2^g, \dots, A_n^g]$ and phases $[P_1^g, P_2^g, \dots, P_n^g]$ of subcarriers are calculated according to their MDS codes for AM $[a_1^g, a_2^g, \dots, a_n^g]$, $a_m^g \in \{1, 2, \dots, A\}$, $m \in \{1, 2, \dots, n\}$, and MDS codes for PM $[p_1^g, p_2^g, \dots, p_n^g]$, $p_m^g \in \{1, 2, \dots, P\}$, which are

$$A_m^g = \sqrt{A a_m^g / (1 + 2 + \dots + A)} = \sqrt{2 a_m^g / (A + 1)}, \quad (6)$$

$$P_m^g = \exp[-j(p_m^g - 1)2\pi/P], \quad (7)$$

respectively. The modulated signals on subcarriers in g -th group $\mathbf{x}_g = [x_1^g, x_2^g, \dots, x_n^g]$ are

$$x_m^g = A_m^g P_m^g, \quad m = 1, 2, \dots, n. \quad (8)$$

Performing the above operations for all groups, we obtain N -dimensional modulated subcarriers $\mathbf{x} = [\mathbf{x}_1, \mathbf{x}_2, \dots, \mathbf{x}_G]^T$.

Table 1 gives an example of bits-to-signals mapping of the proposed MDS-based APM mechanism under $n = 2, A = 2$, and $P = 4$ for a group. In this example, the first input bit "0" is the bit for AM whose MDS codes are (1,1). According to (6), the amplitudes decided by MDS codes (1,1)

TABLE I: An example of the proposed MDS-based APM, $n=2, A=2, P=4$

Input bits	AM bits	MDS codes	Amplitude	Modulation signals
	0	(1,1)	$(\sqrt{2/3}, \sqrt{2/3})$	
100	PM bits	MDS codes	Phase	$(\sqrt{\frac{2}{3}}e^{-j\frac{3\pi}{2}}, \sqrt{\frac{2}{3}}e^{-j\frac{\pi}{2}})$
	10	(3,1)	$(e^{-j\frac{3\pi}{2}}, e^{-j\frac{\pi}{2}})$	

are $(\sqrt{\frac{2}{3}}, \sqrt{\frac{2}{3}})$. Similarly, the last two bits “10” are the bits for PM and their corresponding MDS codes are (3,1). Then the phases of the two subcarriers are calculated by (7) and the results are $(e^{-j\frac{3\pi}{2}}, e^{-j\frac{\pi}{2}})$. The modulation signals are $(\sqrt{\frac{2}{3}}e^{-j\frac{3\pi}{2}}, \sqrt{\frac{2}{3}}e^{-j\frac{\pi}{2}})$ according to (8).

B. Discrete RIS Channel Model

The RIS is placed near the RF source so that the fading between the RF source and the RIS is ignorable. The signals passing through the RIS channels can be described as

$$[\mathbf{s}_1, \mathbf{s}_2, \dots, \mathbf{s}_F]^T = [\mathbf{R}_1\mathbf{x}, \mathbf{R}_2\mathbf{x}, \dots, \mathbf{R}_F\mathbf{x}]^T. \quad (9)$$

It is worth noting that the reflectors in the RIS only alter the signal phases but can not affect signal amplitudes. Denoting the phase shift of \mathbf{R}_i at time slot t as θ_{it} , the i -th phase shift matrix can be described as $\mathbf{R}_i = \text{diag}[e^{j\theta_{i1}}, e^{j\theta_{i2}}, \dots, e^{j\theta_{iN}}]$.

This paper focuses on the RIS with limited phase shifts, meaning that the RIS phase shift can only be selected from a set with limited values. Assuming there are Q discrete phase shifts, the set of all alternative discrete phase shifts $\theta = [\theta^1, \theta^2, \dots, \theta^Q]$ are calculated by

$$\theta^q = 2\pi(q-1)/Q, \quad q = 1, 2, \dots, Q. \quad (10)$$

III. DERIVATION FOR OPTIMAL DISCRETE PHASE SHIFTS

This section formulates the PEP of the proposed system and derives the optimal discrete RIS phase shifts to minimize the PEP. From the MDS based APM scheme, we can conclude that there are a total of $(AP)^{n-1}$ combinations for each group. Assuming $\mathbf{x}_a, \mathbf{x}_b \in \mathbb{C}^{n \times 1}$ are two different combinations in one group, the conditional PEP between them is

$$P(\mathbf{x}_a \rightarrow \mathbf{x}_b | \mathbf{h}_r) = Q \left(\sqrt{\frac{\|(\mathbf{X}_a - \mathbf{X}_b)\mathbf{h}_r\|^2}{2N_0}} \right), \quad a \neq b, \quad (11)$$

where $\mathbf{h}_r = [\sum_{i=1}^F h_{it_1} r_{it_1}, \sum_{i=1}^F h_{it_2} r_{it_2}, \dots, \sum_{i=1}^F h_{it_n} r_{it_n}]^T$ denotes the equivalent channel experienced by one group at time frame $\mathbf{t} = [t_1, t_2, \dots, t_n]^T$. $\mathbf{X}_a = \text{diag}[\mathbf{x}_a]$ and $\mathbf{X}_b = \text{diag}[\mathbf{x}_b]$. $Q(\cdot)$ is the Q -function with an approximate expression

$$Q(x) \approx \frac{1}{12}e^{-x^2/2} + \frac{1}{4}e^{-2x^2/3}. \quad (12)$$

Substituting (12) into (11) and calculating the expectation of $P(\mathbf{x}_a \rightarrow \mathbf{x}_b | \mathbf{h}_r)$, we obtain the following approximate unconditional PEP expression as in [9]:

$$P(\mathbf{x}_a \rightarrow \mathbf{x}_b) = \frac{1}{12\det(\mathbf{I}_N + \frac{\mathbf{C}\mathbf{W}_{ab}}{4N_0})} + \frac{1}{4\det(\mathbf{I}_N + \frac{2\mathbf{C}\mathbf{W}_{ab}}{3N_0})}, \quad (13)$$

where \mathbf{I}_n denotes the n -dimensional unit diagonal matrix, $\mathbf{W}_{ab} = (\mathbf{X}_a - \mathbf{X}_b)^H(\mathbf{X}_a - \mathbf{X}_b)$ is a positive semi-definite diagonal matrix which is not related to the RIS, and $\mathbf{C} = E[\mathbf{h}_r\mathbf{h}_r^H]$ is also a positive semi-definite diagonal matrix. Since N_0 is also independent of the RIS, the PEP is minimized only

when $\mathbf{h}_r\mathbf{h}_r^H$ is maximized. Denoting the frequency response of the i -th channel and i -th RIS phase shift at time slot t as $\beta_{it}e^{-j\varphi_{it}}$ and $e^{j\theta_{it}}$, respectively, we further expand $\mathbf{h}_r\mathbf{h}_r^H$ into the following matrix form:

$$\mathbf{h}_r\mathbf{h}_r^H = \begin{bmatrix} \sum_{i=1}^F \sum_{k=1}^F \beta_{it_1}\beta_{kt_1} e^{-j[(\varphi_{it_1}-\theta_{it_1})-(\varphi_{kt_1}-\theta_{kt_1})]} \\ \sum_{i=1}^F \sum_{k=1}^F \beta_{it_2}\beta_{kt_2} e^{-j[(\varphi_{it_2}-\theta_{it_2})-(\varphi_{kt_2}-\theta_{kt_2})]} \\ \vdots \\ \sum_{i=1}^F \sum_{k=1}^F \beta_{it_N}\beta_{kt_N} e^{-j[(\varphi_{it_N}-\theta_{it_N})-(\varphi_{kt_N}-\theta_{kt_N})]} \end{bmatrix}. \quad (14)$$

As we can learn from (14), when all diagonal elements of the obtained matrix reach their maximum values, $\mathbf{h}_r\mathbf{h}_r^H$ is maximized. Hence, the optimization objective is

$$\max_{\{\mathbf{R}_i\}} \sum_{i=1}^F \sum_{k=1}^F \beta_{it}\beta_{kt} e^{-j[(\varphi_{it}-\theta_{it})-(\varphi_{kt}-\theta_{kt})]}, \quad t = t_1, t_2, \dots, t_n. \quad (15)$$

In (15), the maximum value of $e^{-j[(\varphi_{it}-\theta_{it})-(\varphi_{kt}-\theta_{kt})]}$ is 1 when $(\varphi_{it} - \theta_{it}) - (\varphi_{kt} - \theta_{kt}) = 0$. That is, when the RIS phase shifts at every time slot satisfy $\varphi_{it} - \theta_{it} = \varphi_{kt} - \theta_{kt}$, (14) is maximized. The above requirements are not difficult to be satisfied if the phase shifts are continuous. However, the practical RIS with discrete phase shifts is incapable of satisfying $\varphi_{it} - \theta_{it} = \varphi_{kt} - \theta_{kt}$ at almost every time slot, yielding phase shift errors. In such a situation, we need to search the best combination of F discrete phase shifts to maximize (14) among all combinations. In other words, the optimal discrete phase shifts can be obtained by solving

$$\begin{cases} \text{argmax}_{\{\theta_t\}} \sum_{i=1}^F \sum_{k=1}^F \beta_{it}\beta_{kt} e^{-j[(\varphi_{it}-\theta_{it})-(\varphi_{kt}-\theta_{kt})]} \\ \text{s. t. } \theta_{it}, \theta_{kt} \in \theta, \end{cases} \quad (16)$$

where $\theta_t = [\theta_{1t}, \theta_{2t}, \dots, \theta_{Ft}]^T$ is the combination of F phase shifts at time slot t

IV. ALGORITHM FOR OPTIMAL DISCRETE PHASE SHIFTS

A. Simplified Searching Algorithm

This section develops a simplified algorithm to search the optimal combination of discrete phase shifts. Note that based on (14), we can obtain the following expression of the optimal successive RIS phase shifts:

$$(\varphi_{it} - \theta_{it}) = (\varphi_{kt} - \theta_{kt}) = \mu, \quad (17)$$

where $\mu \in [0, 2\pi)$ is an arbitrary real number. Note that (17) only requires the phases of F paths to be equal, but does not limit the value of μ . With the change of μ , the optimal combination alters. Therefore, there are more than one optimal combinations that can minimize PEP. Analogously to the analysis of successive phase shifts, we assert that the optimal combinations of discrete RIS phase shifts are also more than one. However, when searching the optimal combinations, it is unnecessary to find all of them. Instead, one optimal combination is enough. Based on the above analyses, we propose a simplified searching algorithm in **Algorithm 1**. We first set $\mu = 0$ to calculate one optimal combination of continuous phase shifts. Then we calculate two discrete phase shifts that are closest to the optimal continuous phase shift for each path, which are denoted as θ_{ih} and θ_{il} , respectively.

Algorithm 1: Optimal discrete RIS phase shifts

Input: N ; Q ; F ; time domain paths $\mathbf{h}_1, \mathbf{h}_2, \dots, \mathbf{h}_F$
Output: Discrete RIS phase shift matrixs of F paths

 $\mathbf{R}_1, \mathbf{R}_2, \dots, \mathbf{R}_F$

```

1 for  $t = 1 : N$  do
2   for  $i = 1 : F$  do
3      $\varphi_i(t) = \theta_i(t)$ ;
4      $\theta_{ih} = \frac{2\pi}{Q} \lceil \frac{\varphi_i(t)}{2\pi/Q} \rceil$ ,  $\theta_{il} = \frac{2\pi}{Q} \lfloor \frac{\varphi_i(t)}{2\pi/Q} \rfloor$ ;
5   for  $\theta_{it} = [\theta_{ih}, \theta_{il}]$ ,  $\theta_{kt} = [\theta_{kh}, \theta_{kl}]$  do
6      $\theta_i(t) = \operatorname{argmax}_{\{\theta_t\}} \sum_{i=1}^F \beta_{it} \beta_{kt} e^{-j[(\varphi_{it} - \theta_{it}) - (\varphi_{kt} - \theta_{kt})]}$ 
7 for  $i = 1 : F$  do
8   return  $\mathbf{R}_i = \operatorname{diag}[e^{j\theta_i(1)}, e^{j\theta_i(2)}, \dots, e^{j\theta_i(N)}]$ 

```

TABLE II: An example of **Algorithm 1**, Rayleigh channels, $F = 2$, $Q = 8$

	Frequency domain channel	Optimal successive phase shift	$\theta_{ih} \theta_{il}$	Optimal discrete phase shift
\mathbf{R}_1	$-4.5962 - 2.0222j$	1.8674π	$\frac{7\pi}{4} \ 0$	$\frac{7\pi}{4}$
\mathbf{R}_2	$0.9819 + 1.1333j$	0.7273π	$\frac{2\pi}{4} \ \frac{3\pi}{4}$	$\frac{3\pi}{4}$

We further calculate the objective in (16) with all the possible combinations of θ_{ih} and θ_{il} and one optimal combination θ_i must be in these combinations.

Furthermore, we give an example of **Algorithm 1** in Table 2. In this example, 2 programmable reflectors and 8 discrete phase shifts are adopted. According to (10), the set of all discrete phase shifts is $\{0, \frac{\pi}{4}, \frac{2\pi}{4}, \frac{3\pi}{4}, \pi, \frac{5\pi}{4}, \frac{6\pi}{4}, \frac{7\pi}{4}\}$. We first calculate the phases of the two channels and assign them as the optimal successive phase shifts, which are 1.8674π and 0.7273π , respectively. Then, the pairs θ_{1h}, θ_{2h} and θ_{1l}, θ_{2l} are achieved. To be concrete, we have $\theta_{1h} = \frac{7\pi}{4}$, $\theta_{2h} = 0$ and $\theta_{1l} = \frac{2\pi}{4}$, $\theta_{2l} = \frac{3\pi}{4}$. Then, 4 candidate combinations are obtained, which are $(\frac{7\pi}{4}, \frac{2\pi}{4})$, $(\frac{7\pi}{4}, \frac{3\pi}{4})$, $(0, \frac{2\pi}{4})$ and $(0, \frac{3\pi}{4})$. Finally, we plug each combination into (16) and obtain 4 results. The combination with the maximum result is the optimal solution. In this example, it is $\frac{7\pi}{4}, \frac{3\pi}{4}$.

B. Complexity Analysis

The complexity order of conventional searching algorithm for (16) is

$$C = Q^F + 2F^2Q^F = Q^F(1 + 2F^2), \quad (18)$$

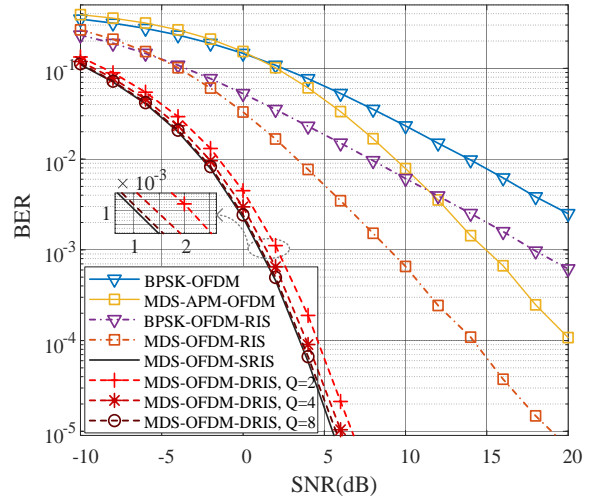
which grows exponentially with both Q and F . And the complexity order of the proposed searching algorithm is

$$C' = 2^F + 2F^2 \times 2^F = 2^F(1 + 2F^2). \quad (19)$$

Although C' still grows exponentially with F , it is no longer impacted by Q . And the proposed algorithm reduces the calculation complexity without any performance loss.

V. SIMULATION RESULTS

This section provides numerical results to verify the performance of the proposed MDS-OFDM system over the RIS channels (MDS-OFDM-RIS). In simulations, we first set $N = 256$, $G = 128$, $n = 2$, $A = 2$, and $P = 2$ so that the length of information bits is $L = 128 \times (2 - 1) \times \log_2(2 \times 2) = 256$ and the transmission rate T_r is 1bps . The simulation results are

Fig. 2. BER comparisons when $n = 2$, $A = 2$, $P = 2$, $F = 4$, $T_r = 1\text{bps}$.

shown in Fig. 2, where the number of reflective elements is 4. The wireless channel models are independent and identically distributed time-varying Rayleigh fading channels. We assume the RIS knows the channel information and [15] proves that such an assumption is feasible. In this Section, MDS-APM-OFDM denotes the proposed MDS-APM based OFDM system. RIS, SRIS and DRIS represent the non-optimal RIS, optimal successive RIS and optimal discrete RIS, respectively.

In Fig. 2, the proposed MDS-APM-OFDM system outperforms BPSK-OFDM when SNR is higher than 0 dB. Specifically, it provides a gain of 5 dB at the BER of 10^{-2} . However, when the transmission environment is poor, the BER performance of MDS-APM-OFDM system is slightly worse than that of BPSK-OFDM. Such a phenomenon occurs because high noise may bring a negative impact on the error detection ability of MDS codes. With the increase of SNR, the advantages of MDS-APM becomes more prominent. As can be seen from Fig. 2, when the SNR is 20 dB, the BER of the MDS-APM-OFDM system is reduced to 10^{-4} , while the BER of the BPSK-OFDM system is still higher than 10^{-3} .

The RIS is employed to BPSK-OFDM and MDS-APM-OFDM in order to achieve further performance improvement. To be specific, it offers a gain of 6 dB at the BER of 10^{-2} for both BPSK-OFDM and MDS-APM-OFDM. It can be further found from Fig. 2 that MDS-APM-OFDM obtains more performance gain at low SNR regions because of the link enhancement function of RIS.

In Fig. 2, the curve of the MDS-OFDM-SRIS system is the ideal case, but it is unreachable since continuous phase shifts are unrealizable. As can be observed, in accordance with the analysis in Section III, discrete phase shifts cause BER performance loss. And the performance loss decreases with the increase of Q . More specifically, the performance loss is 1.1 dB and 0.4 dB at the BER of 10^{-3} for $Q = 2$ and $Q = 4$, respectively. When Q increases to 8, the BER performance of the proposed method becomes very close to the optimum in the whole SNR regime, where the performance loss keeps lower than 0.1 dB. Even better, the increase of Q has almost no effect on the calculation complexity.

We further conduct simulations to test the system BER when more information bits are carried. In Fig. 3, we set $n = 2$, $A = 4$, and $P = 4$. This increases the transmission rate to 2bps so that 512 information bits are sent. As can be seen, although

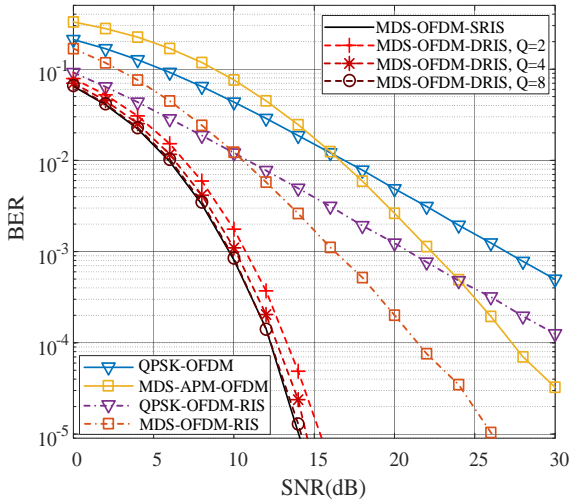


Fig. 3. BER comparisons when $n = 2$, $A = 4$, $P = 4$, $F = 4$, $T_r = 2\text{bps}$.

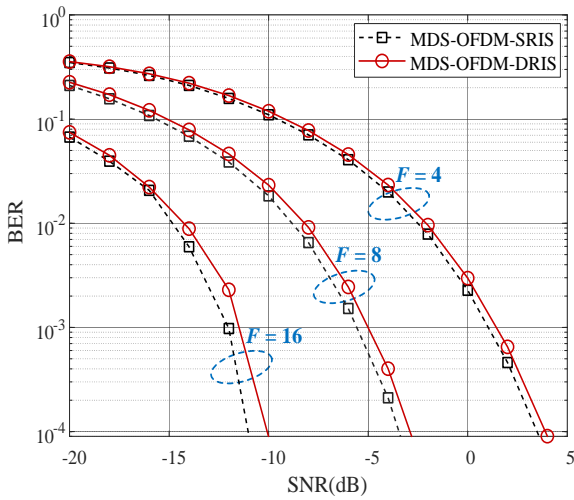


Fig. 4. BERs of MDS-OFDM-SRIS and MDS-OFDM-DRIS when F is 4, 8 and 16.

the modulation orders are changed, the variation trends of the curves in Fig. 3 keep consistent with those in Fig. 2. The increase of modulation orders shortens the distance between modulation symbols, pushing the advantage of MDS code to higher SNRs. This problem can be easily solved by introducing and optimizing the RIS, as demonstrated in Fig. 3.

In Figs. 2 and 3, F is set to be a constant value. It is not certain that whether the number of reflectors affects the system BER. For this reason, we further simulate the BERs of the proposed MDS-OFDM-DRIS and MDS-OFDM-SRIS systems under different value of F and the results are shown in Fig. 4, where $Q = 4$. As can be seen in Fig. 4, the BER performance increases when more reflectors are used. Besides, the BERs of the MDS-OFDM-DRIS systems keep close to that of MDS-OFDM-SRIS systems under different value of F , indicating that optimal discrete phase shifts are adaptable to the change of F .

VI. CONCLUSION

This paper has proposed a novel MDS-coded OFDM-RIS system for improving the BER performance. By considering practical discrete RIS phase shifts, performance loss of system BER was observed and compared with continuous phase shifts. The PEP of the proposed system was first formulated and

the optimal discrete RIS phase shifts were then derived. The proposed system has been demonstrated to provide a considerable improvement on system BER performance compared with conventional OFDM systems. The proposed framework can be a new and practical candidate paradigm for 6G.

REFERENCES

- [1] C. Wang, J. Huang, H. Wang, X. Gao, X. You, and Y. Hao, "6G wireless channel measurements and models: Trends and challenges," *IEEE Veh. Technol. Mag.*, vol. 15, no. 4, pp. 22-32, Dec. 2020.
- [2] A. Yazar and H. Arslan, "A waveform parameter assignment framework for 6G with the role of machine learning," *IEEE Open J. Veh. Technol.*, vol. 1, pp. 156-172, May. 2020.
- [3] F. Aoudia and J. Hoydis, "Waveform learning for next-generation wireless communication systems," *IEEE Trans. Commun.*, vol. 70, no. 6, pp. 3804-3817, Jun. 2022.
- [4] X. Chen, Z. Feng, Z. Wei, P. Zhang, and X. Yuan, "Code-division OFDM joint communication and sensing system for 6G machine-type communication," *IEEE Internet Things J.*, vol. 8, no. 15, pp. 12093-12105, Aug. 2021.
- [5] Y. Wang, Z. Wei, W. Zhou, K. Han, and Z. Feng, "Triangular FM-OFDM waveform design for integrated sensing and communication," *ICC Workshops*, Seoul, Korea, 2022, pp. 515-519.
- [6] F. Yarkin and J. Coon, "Q-Ary multi-mode OFDM with index modulation," *IEEE Wireless Commun. Lett.*, vol. 9, no. 7, pp. 1110-1114, Jul. 2020.
- [7] S. Negusse, P. Zetterberg, and P. Handel, "Phase-noise mitigation in OFDM by best match trajectories," *IEEE Trans. Commun.*, vol. 63, no. 5, pp. 1712-1725, May. 2015.
- [8] H. Zhang, L. Zhang, Y. Jiang, and Z. Wu, "Reliable and secure deep learning-based OFDM-DCSK transceiver design without delivery of reference chaotic sequences," *IEEE Trans. Veh. Technol.*, vol. 71, no. 8, pp. 8059-8074, Aug. 2022.
- [9] E. Basar, U. Aygolu, E. Panayirci, and H. Poor, "Orthogonal frequency division multiplexing with index modulation," *IEEE Trans. Signal Process.*, vol. 61, no. 22, pp. 5536-5549, Nov. 2013.
- [10] L. Zhao, Y. W. Chen, W. Zhou, R. K. Shiu, S. Shen, Y. Lu, J. Yu, and G. K. Chang, "Polar coded OFDM signal transmission at the W-band in Millimeter-wave system," *IEEE Photonics J.*, vol. 11, no. 6, pp. 1-6, Dec. 2019.
- [11] F. Yarkin and J. Coon, "Modulation based on a simple MDS code: Achieving better error performance than index modulation and related schemes," *IEEE Trans. Commun.*, vol. 70, no. 1, pp. 118-131, Jan. 2022.
- [12] F. Yarkin and J. Coon, "Simple gray coding and LLR calculation for MDS modulation systems," *IEEE WCNC*, Austin, TX, USA, 2022, pp. 268-273.
- [13] M. Renzo, A. Zappone, M. Debbah, M. Alouini, C. Yuen, J. Rosny, and S. Tretjakov, "Smart radio environments empowered by reconfigurable intelligent surfaces: How it works, state of research, and the road ahead," *IEEE J. Sel. Areas Commun.*, vol. 38, no. 11, pp. 2450-2525, Nov. 2020.
- [14] C. Pradhan, A. Li, L. Song, J. Li, B. Vucetic, and Y. Li, "Reconfigurable intelligent surface (RIS)-enhanced two-way OFDM communications," *IEEE Trans. Veh. Technol.*, vol. 69, no. 12, pp. 16270-16275, Dec. 2020.
- [15] E. Basar, M. Di Renzo, J. De Rosny, M. Debbah, M. S. Alouini, and R. Zhang, "Wireless communications through reconfigurable intelligent surfaces," *IEEE Access*, vol. 7, pp. 116753-116773, Aug. 2019.
- [16] S. Lin, B. Zheng, G. Alexandropoulos, M. Wen, F. Chen, and S. Mumtaz, "Adaptive transmission for reconfigurable intelligent surface-assisted OFDM wireless communications," *IEEE J. Sel. Areas Commun.*, vol. 38, no. 11, pp. 2653-2665, Nov. 2020.
- [17] P. Xu, G. Chen, Z. Yang, and M. Renzo, "Reconfigurable intelligent surfaces-assisted communications with discrete phase shifts: How many quantization levels are required to achieve full diversity," *IEEE Wireless Commun. Lett.*, vol. 10, no. 2, pp. 358-362, Feb. 2021.
- [18] H. Zhang, B. Di, L. Song, and Z. Han, "Reconfigurable intelligent surfaces assisted communications with limited phase shifts: How many phase shifts are enough," *IEEE Trans. Veh. Technol.*, vol. 69, no. 4, pp. 4498-4502, Apr. 2020.
- [19] K. Katsanos, N. Shlezinger, M. Imani, and G. Alexandropoulos, "Wideband multi-user MIMO communications with frequency selective RISs: Element response modeling and sum-rate maximization," *IEEE ICC Workshops*, Seoul, South Korea, 2022, pp. 151-156.
- [20] K. Katsanos, P. Lorenzo, and G. Alexandropoulos, "Distributed sum-rate maximization of cellular communications with multiple reconfigurable intelligent surfaces," *IEEE SPAWC*, Oulu, Finland, 2022, pp. 1-5.